*Ferroelectrics*, 2001, Vol. 253, pp. 105-114
Reprints available directly from the publisher
Photocopying permitted by license only



# Formation of Self-Organized Nanodomain Patterns During Spontaneous Backswitching in Lithium Niobate

V.YA. SHUR[a]*, E.L. RUMYANTSEV[a], E.V. NIKOLAEVA[a], E.I. SHISHKIN[a], D.V. FURSOV[a], R.G. BATCHKO[b], L.A. EYRES[b], M.M. FEJER[b], R.L. BYER[b] and J. SINDEL[c]

[a]*Inst. Phys.& Appl. Math., Ural State University, Lenin Ave. 51, 620083 Ekaterinburg, Russia;* [b]*E.L. Ginzton Laboratory, Stanford University, Stanford, CA 94305;* [c]*Materials Research Lab, The Pennsylvania State University, University Park, PA 16802-4800*

*(Received June 2, 2000)*

We show experimentally that spontaneous decay of highly non-equilibrium domain state in ferroelectric is achieved through the formation of self-organized nanoscale domain structures. The nanodomain structures have been observed by SEM and SFM in uniaxial ferroelectric lithium niobate during spontaneous backswitching after fast removing of switching field. The regular nanoscale domain patterns consist of strictly oriented arrays of nanodomains (diameter down to 30 nm, density up to 100 $\mu m^{-2}$). The mechanisms of self-maintaining correlated nucleation effects are discussed.

*Keywords*: domain engineering; nanotechnology; domain structure; kinetics; switching

* Corresponding author. E-mail: vladimir.shur@usu.ru

## INTRODUCTION

It is well known that the self reversal effect or "elastic" switching occurs in certain ferroelectric materials.[1,2] When the switching pulse is applied a certain amount of polarization reversal occurs; however as soon as the pulse is completed the created domain structure becomes unstable and material spontaneously relaxes back to very nearly its initial domain state.[3-5] It was shown that the characteristic time of this process strongly depends on material, temperature and parameters of the switching pulse.[3-5] The investigation of these effects is usually based on analysis of the switching current data. To our knowledge the visualization of the domain evolution during this spontaneous decay (backswitching or flip-back) have not been carried out.

## EXPERIMENT

The spontaneous decay of the domain structure was investigated in standard optical-grade 0.5-mm-thick wafers of congruent $LiNbO_3$ cut normal to polar axis. The wafers were photolithographically patterned with periodic strip metal-electrode structure (NiCr) deposited on polar surface only. The electrodes were oriented along one of **Y** directions. The patterned surface was covered by a thin (about 1 μm-thick) insulating layer (photoresist or spin-on-glass)(Fig. 1a). A high voltage pulse was applied to the structure through the fixture containing a liquid electrolyte (LiCl).[6,7] The voltage waveform contains three main stages: high-field, low-field, and stabilization-field (Fig. 1b). The switching takes place at the high-field stage and the backswitching occurs during the low-field one. The stabilization-field stage freezes-in the domain pattern existing at the end of backswitching stage. The comparison of the domain patterns obtained for different duration of the low-field stage yields the information about the development of the domain structure during backswitching. For observation of the domain patterns the polar surfaces polished after controlled backswitching were etched for 5 to 10 minutes by hydrofluoric acid (without heating). The high-resolution scanning microscopes SEM and SFM have been used for investigation of the surface relief.

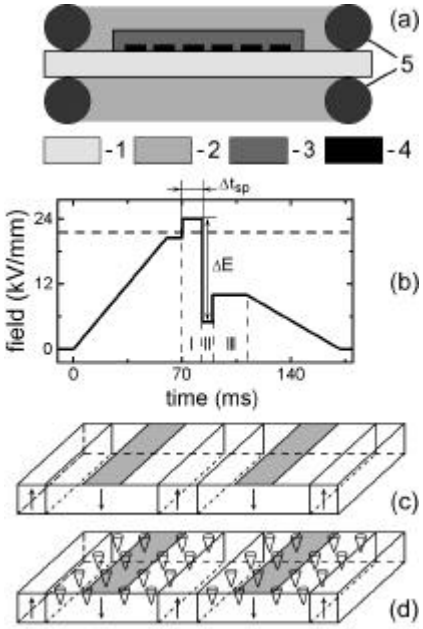


FIGURE 1 (a) Scheme of experimental setup: 1 - $LiNbO_3$ wafer, 2 - liquid electrolyte, 3 - insulating layer, 4 - periodic metal electrodes, 5 - O-rings. (b) The voltage waveform: I - high-field stage, II - low-field stage, III - stabilization stage. The schematic drawings of domain patterns corresponding to the end of (c) high-field stage and (d) low-field stage.

## EVOLUTION OF THE DOMAIN STRUCTURE

Switching from the initial single-domain state starts when applied field exceeds threshold value for quasi-static switching ($E_{th}$ = 21.0 kV/mm)[8] (Fig. 1b). The periodic laminar domains created during high-field stage are always wider than the electrodes (domain spreading) (Fig. 1c).[6,7,9]

We have discovered that evolution of domains in $LiNbO_3$ during backswitching is a highly organized process.[10] This spontaneous decay of laminar domain structure proceeds through arising and growth of oriented nanoscale domain arrays (Fig. 1d) contrary to expected trivial backward motion of the existing domain walls accompanied by

random nucleation of new domains. Such parameters of voltage waveform as the duration of the high-field stage $\Delta t_{sp}$ and the value of the jump from high to low field (field-diminishing amplitude) $\Delta E$ allow to control the backswitching kinetics. Three main scenarios of the highly organized domain evolution have been revealed (Fig. 2-4).

## NANODOMAIN PATTERNS

In the samples with large period of electrode structure (more than 8 μm) for long switching pulse $\Delta t_{sp}$ ~ 15 ms the wall shift out of

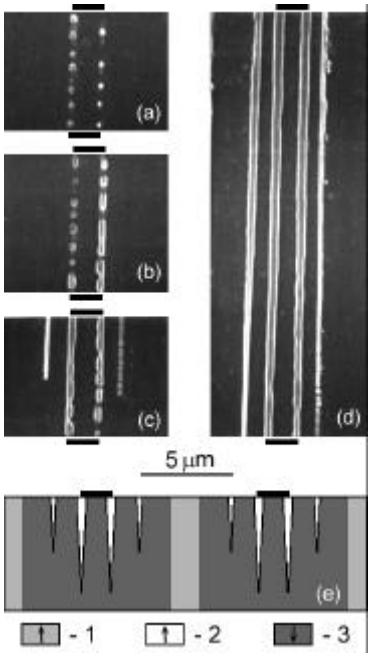


FIGURE 2 (a - d) SEM domain patterns demonstrating the stages of the formation of periodic strip backswitched domains oriented along the electrode edges. Top view. Black rectangles show the positions of the electrodes. (e) The cross-section of domain pattern corresponding to stage (d) (schematical illustration). 1 - non-switched domains, 2 - backswitched domains, 3 - switched domains.

electroded area exceeds 3 μm. For high field-diminishing amplitude ΔE ~ 20 kV/mm the backswitching leads to the formation of the periodic strip domains oriented along the electrodes (Fig. 2d). The process starts with arising of the couple of 1D-nanodomain arrays strictly under the electrode edges (Fig. 2a). The image processing demonstrates the strong correlation of spatial distribution of nanodomains (average distance between neighbors is about 200 nm). These arrays turn into a pair of strip domains through growth and merge of nanodomains (Fig. 2b). Then the new couple of 1D arrays appears in nonelectroded area parallel to the first ones at the distance about 1 μm (Fig. 2c) and forms a new pair of strip domains (Fig. 2d).

The domain patterns for electrode periods less than 4 μm are highly organized quasi-periodical structure of nanodomain arrays oriented along crystallographic directions (Fig. 3 and 4). Two variants of array orientation have been obtained. For short switching pulse

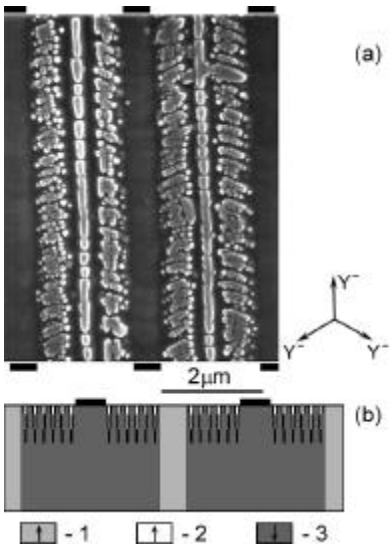


FIGURE 3 (a) SEM nanodomain patterns with arrays oriented along **Y**⁻ directions. Top view. (b) The scheme of domain pattern cross-section.

duration $\Delta t_{sp}$ ~ 5 ms and low field-diminishing amplitude $\Delta E$ ~ 2 kV/mm the domain arrays are oriented strictly in one of three $\mathbf{Y}^{-}$ directions (Fig. 3) at 60 degrees to the electrode edges.

Each array is comprised of domains with diameters 30-100 nm and average linear density exceeding $10^4 mm^{-1}$. The nucleation under the electrode has been never observed (Fig. 3a). For $\Delta E$ > 30 kV/mm (change of the field sign) the domain arrays are oriented strictly in one of six **X** directions (Fig. 4). The individual nanoscale domains are triangular shaped and their sizes are ranged from 30 to 100 nm. In addition the nucleation along the electrode edges and consequent formation of strip domains is observed.

All observed results can be explained under the preposition that switching process in the given place is driven by the local electric field

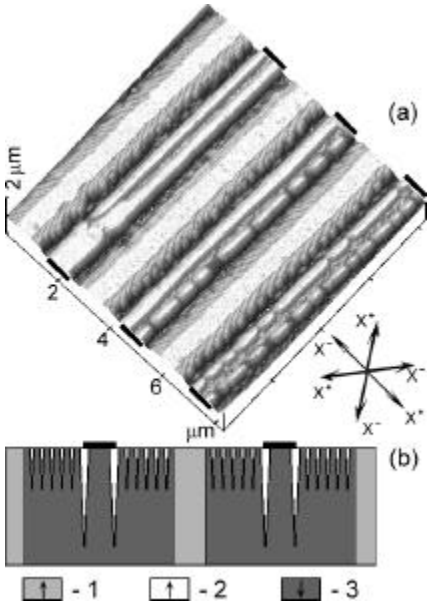


FIGURE 4 (a) SFM nanodomain patterns with arrays oriented along **X** directions. Top view. (b) The scheme of domain pattern cross-section.

$E_z$, which depends on the instantaneous domain pattern and screening degree.[11-13] $E_z$ is defined by the sum of the polar component of external field $E_{ex}$, depolarization field $E_{dep}$ and various screening fields $E_{scr}$.

$$E_z(r,t) = E_{ex}(r) - E_{dep}(r,t) - \Sigma E_{scr}(r,t) \quad (1)$$

In the case of strip electrodes $E_{ex}$ strongly increases in the surface layer along the electrode edges due to the fringe effect. The depolarization nanoscale domains are triangular shaped and their sizes are about 30-100 nm. In addition the nucleation along the electrode edges and consequent formation of strip domains is observed.

$E_{dep}$ arising during switching is rapidly screened mainly by the current in the external circuit (external screening). The residual part of

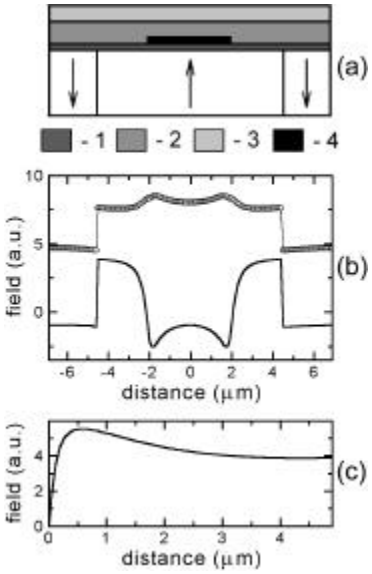


FIGURE 5 (a) Substrate surface region with strip electrode: 1 - dielectric gap, 2 - insulating layer, 3 - liquid electrolyte, 4 - metal electrode and (b) calculated spatial distribution of backswitching field at the low-field stage near $\mathbf{Z}^+$ surface (solid line - low $\Delta E$ and short $\Delta t_{sp}$, circles - $\Delta E > 30$ kV/mm). (c) Calculated change of $E_z$ near the domain wall at the surface.

depolarization field $E_{rdep}$ depends on the ratio between thickness of sample d and dielectric layer L (Fig. 5a).[14]

$$E_{rdep} = L\ P_s/\varepsilon\varepsilon_o\ d \qquad (2)$$

Under the electrodes the thickness of dielectric layer is determined by the sub-micron intrinsic layer (dead layer) $L_{in}$, while out of electrodes by deposited isolating layer (about 1 μm) $L_{is}$. So $E_{rdep}$ under the electrodes is much less than in out-of-electroded area as $L_{in} << L_{is}$ (Fig. 5a). The residual part of the local field $E_{zr}(r,t) = E_{ex}(r) - E_{rdep}(r,t)$ is compensated by bulk screening, which is much slower (for $LiNbO_3$ at RT the time constant is about 10-30 ms[6,9,15]) than external one. It is determined by redistribution of bulk charges, reorientation of defect dipoles and injection from electrodes through the insulating layer during switching. [12,14,16]

After removing/diminishing of external field the backswitching occurs under the action of depolarization field and the field produced by the charges, which were screening external field at high-field stage. $E_{rdep}$ prevails in backswitching in out-of-electroded-area and its value decreases on switching time. In contrast the bulk screening of external field increases on switching time. The inhomogeneous field produced by the bulk screening charges initiates the backswitching under the electrodes. Thus the spatial distribution of backswitching field depends on $\Delta t_{sp}$ and $\Delta E$.

Within this approach the first scenario (Fig. 2) is due to complete screening of the $E_{rdep}$ and backswitching occurs only under the action of screening charges, which have been compensating the external field. The field maximums existing along the electrode edges determine the position of the first arrays. The calculation shows that at the distance about the depth of the intrinsic dielectric gap or insulating layer from any arising backswitched domain the pronounced maximums of $E_z$ is formed in the surface layer thus determining the position of subsequent nuclei (Fig. 5c). This approach explains the fact that observed distance between nanodomain arrays in this case is about the depth of insulating layer. This effect leads also to the self-consistent nucleation within array, which results in formation of correlated structure.

According to our estimations (Fig. 5b) of the spatial distributions of backswitching field the second scenario corresponds to the case when depolarization field prevails (Fig. 5b, curve I) and backswitching occurs only in out-of-electroded area (Fig. 3). Third scenario (Fig. 4) is realized for $\Delta E > E_{ex}$. The inverse external field applied during the low-field stage provides the backswitching as under, so out of the electrodes (Fig. 5b, curve II).

The developing process of correlated nucleation represents the self-maintaining generation of the parallel arrays (Fig. 3 and 4). This effect is of the same origin as the discussed above formation of the arrays along the electrode edges (Fig. 2). The existing at the given moment array-aggregate generates the new maximum of backswitching field at the fixed distance in front of its boundary and triggers the arising of new array. The array-assisted growth of the correlated domain structure is similar to the formation of "wide domain boundary" discovered by us in $Pb_5Ge_3O_{11}$.[17] Such growth leads to superfast polarization reversal by the fast spreading of the ordered structure consisting of the oriented arrays of nanodomains.

The array orientation strictly along crystallographic directions is an evidence of anisotropy of nucleation kinetics in $LiNbO_3$ in such highly nonequilibrium state. We have observed the similar formation of the oriented micro-domain arrays in $LiNbO_3$ during polarization reversal in strong homogeneous field.[9]

## CONCLUSION

In summary, we have reported the first observation of spontaneous decay of the highly nonequilibrium ferroelectric domain state. We have shown that backswitching in $LiNbO_3$ is accomplished through the formation of the self-organized nanoscale domain arrays. The experimental evidence of self-maintained highly anisotropic nucleation kinetics has been presented. The simulated spatially nonuniform field distribution arising and varying during domain evolution have been invoked for explanation of obtained results. The observed avalanche nucleation drastically enhances the switching rate (the velocity of expansion of switched area).

ACKNOWLEDGMENTS

We gratefully acknowledge discussions with Prof. J.F. Scott, Prof. L.A. Shuvalov, and Dr. A.L. Alexandrovsky.

This material is based upon work partially supported by Program "Basic Research in Russian Universities" (Grant No.5563), by Grant of the Ministry of Education of the Russian Federation, by Grant No. 98-02-17562 of RFBR, by DARPA/ONR through the CNOM at Stanford University under ONR Grant No 00014-92-J-1903 and LLNL.

## *References*

[1] E. Fatuzzo and W.J. Merz, *Ferroelectricity* (North-Holland Publishing Company, Amsterdam, 1967), p.201.

[2] J.C. Burfoot and G.W. Taylor, *Polar Dielectrics and their Applications* (University of Calif. Press, Berkeley and Los Angeles, 1979), p.465.

[3] E. Fatuzzo and W.J. Merz, *Phys. Rev.*, **116**, 61 (1959).

[4] G.W. Taylor, *J. Appl. Phys.*, **37**, 593 (1966).

[5] V.Ya. Shur, A.L. Gruverman, V.P. Kuminov, and N.A. Tonkachyova, *Ferroelectrics*, **111**, 197 (1990).

[6] G.D. Miller, R.G. Batchko, M.M. Fejer, and R.L. Byer, in *SPIE Proceedings on Nonlinear Frequency Generation and Conversion*, Vol. 2700 (SPIE, Washington, 1996), p. 34.

[7] V.Ya. Shur, E.L. Rumyantsev, R.G. Batchko, G.D. Miller, M.M. Fejer, and R.L. Byer, *Ferroelectrics*, **221**, 157 (1999).

[8] A.M. Prokhorov and Y.S. Kuzminov, *Physics and Chemistry of Crystalline Lithium Niobate (*Adam Hilger, Bristol, 1990), p.263.

[9] V.Ya. Shur, E.L. Rumyantsev, R.G. Batchko, G.D. Miller, M.M. Fejer, and R.L. Byer, *Phys. Solid State*, **41**, 1681 (1999).

[10] H. Haken, *Rev. Mod. Phys.*, **47**, 67 (1975).

[11] V.Ya. Shur, Yu.A. Popov, and N.V. Korovina, *Sov. Phys. Solid State*, **26**, 471 (1984).

[12] V.Ya. Shur, *in Ferroelectric Thin Films: Synthesis and Basic Properties*, Edited by C.A. Paz de Araujo, J.F. Scott, G.W. Taylor, Vol. 10 (Gordon & Breach Science Publ., 1996), p.153.

[13] V.Ya. Shur and E.L. Rumyantsev, *Ferroelectrics*, **191**, 319 (1997).

[14] V.M. Fridkin, *Ferroelectrics Semiconductors*, (Consultants Bureau, New York and London, 1980).

[15] V. Gopalan, T.E. Mitchell, K.E. Sicakfus, *Sol. St. Commun.*, **109**, 111 (1999).

[16] P.V. Lambeck and G.H. Jonker, *Ferroelectrics*, **22**, 729 (1978).

[17] V.Ya. Shur, A.L. Gruverman, N.Yu. Ponomarev, and N.A. Tonkachyova, *Ferroelectrics*, **126**, 371 (1992).